THE JOURNAL OF PHYSICAL CHEMISTRY C

Article

Cite This: J. Phys. Chem. C XXXX, XXX, XXX−XXX

pubs.acs.org/JPCC

Improving Photovoltaic Stability and Performance of Perovskite Solar Cells by Molecular Interface Engineering

Published as part of The Journal of Physical Chemistry virtual special issue "Abraham Nitzan Festschrift".

Linan Meng,[†,‡] Fan Zhang,[†] Wei Ma,[†,§] Yu Zhao,[†] Peng Zhao,[†] Huixia Fu,[†] Wenlong Wang,[†] Sheng Meng,[*,†,∥] and Xuefeng Guo[*,⊥,#]

[†]Beijing National Laboratory for Condensed Matter Physics, Institute of Physics, Chinese Academy of Sciences, Beijing 100190, People's Republic of China

[‡]University of Chinese Academy of Sciences, Beijing 100049, People's Republic of China

[§]Ningxia Key Laboratory of Photovoltaic Materials, Ningxia University, Yinchuan, Ningxia 750021, People's Republic of China

[∥]Collaborative Innovation Center of Quantum Matter, Beijing 100190, People's Republic of China

[⊥]Beijing National Laboratory for Molecular Sciences, State Key Laboratory for Structural Chemistry of Unstable and Stable Species, College of Chemistry and Molecular Engineering, Peking University, Beijing 100871, People's Republic of China

[#]Department of Materials Science and Engineering, College of Engineering, Peking University, Beijing 100871, People's Republic of China

Supporting Information

ABSTRACT: Interface engineering in perovskite solar cells (PSCs) plays a key role in achieving high-power conversion efficiency (PCE, η) by suppressing electron−hole recombination and facilitating carrier injection. Here we adopt a hydrophobic molecule, 1-donecyl mercaptan (NDM), to modify the interface between $MAPbI_3$ and a hole transport layer (HTL). As a result, an improved PCE of PSCs from 12.75% (pristine $MAPbI_3$) to 15.04% (modified $MAPbI_3$ with NDM) is achieved, along with long-term antimoisture characteristics. First-principles simulations unravel an enhanced driving force for hole injection from $MAPbI_3$ to the HTL upon NDM adsorption, providing atomic-scale insights into the improved PCE. The combined experiment and simulation efforts offer a simple but effective molecular approach to fabricate PSCs with a higher PCE and better moisture tolerance.

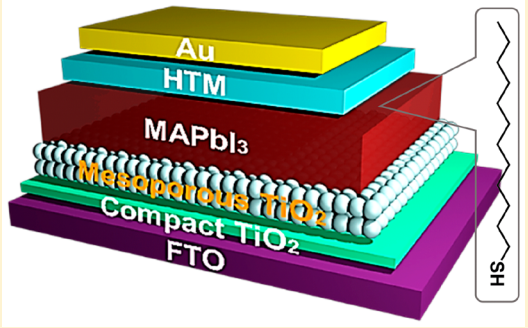

INTRODUCTION

Organic/inorganic trihalide lead-based perovskite materials have been widely employed in solar cells as light absorption and charge transport layers, given their remarkable potential in optoelectronic applications.[1] $MAPbI_3$ perovskite possesses superiorities over other photovoltaic materials, such as easy manufacturing by solution processing,[1,2] strong photon absorption, and long carrier diffusion length (up to micrometers[3−5]). Many efforts have been devoted to engineer perovskite layers to improve the photovoltaic properties of perovskite solar cells (PSCs).[6−10] As a result, the efficiency of perovskite-based solar cells has quickly reached 23.7% in a few years.[11] Although PSCs have made rapid advancement, some challenges still exist for large-scale industrial applications, including the toxicity of Pb and low tolerance against moisture/light/heat.

Among those disadvantages, the instability in the humid environment is a critical issue for its practical large-scale application. $MAPbI_3$ can be easily decomposed upon exposure to moisture in the atmosphere.[12−15] The methylammonium cation ($CH_3NH_3^+$) can diffuse out from the lattice and react with water when exposed to air.[12,13] Generally speaking, there are four routes to improve the antimoisture stability of perovskite films, such as material engineering on the active layer,[1,16,17] optimizing the interface between the active layer and hole transport layer (HTL),[18−21] utilizing inorganic HTL[22−25] materials, and ameliorating morphologies and properties of the surface of the overall device.[26,27] Mohite et al.[8] applied Ruddlesden−Popper phase-layered perovskite films instead of traditional perovskites to improve the intrinsic stability of the active layer. Grätzel et al.[16] modified the surface of methylammonium lead triiodide ($MAPbI_3$) perovskite by spin-coating its precursor solution in the presence of butylphosphonic acid 4-ammonium chloride to improve the performance and stability. Yang et al.[25] replaced the organic HTL by a metal oxide transport layer such as NiO_x, owing to

Received: October 4, 2018
Revised: December 15, 2018
Published: December 24, 2018

DOI: 10.1021/acs.jpcc.8b09722
J. Phys. Chem. C XXXX, XXX, XXX−XXX

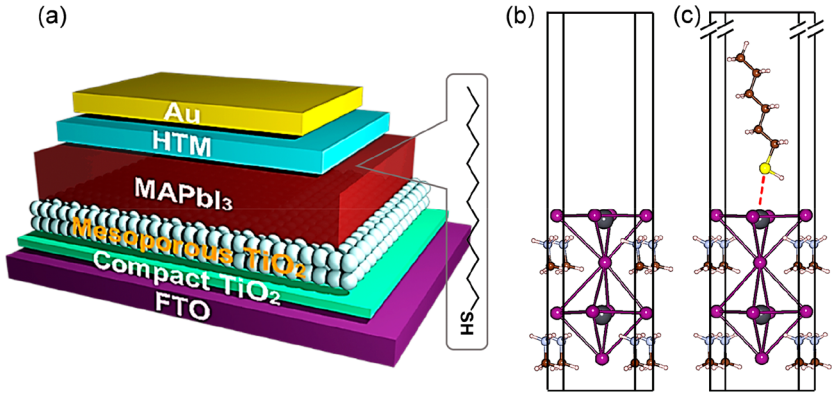

Figure 1. (a) Schematic structure of a PSC, modified by NDM molecules on the interface of $MAPbI_3$ and a HTL. Schematic structure for the surface of pristine $MAPbI_3$ (b) and $MAPbI_3$ anchored with NDM* (c).

its higher carrier mobility and superior stability. Sunkara et al.[10] added graphene−polyaniline into the hole-conducting polymer to minimize the influence of moisture. Using novel materials[7,8] such as Ruddlesden−Popper phase-layered two-dimensional perovskite films might be optimal to improve the stability. Employing metal oxide or other water-repellent materials to the replace spiro-OMeTAD HTL[22−25] is another efficient way to protect the $MAPbI_3$ against humidity. However, the methods mentioned above always lead to an unfavorable drop in energy conversion efficiency. Enhancing the moisture tolerance of $MAPbI_3$ without sacrificing the power conversion efficiency (PCE) at the same time is the focus of the present work.

Here we demonstrate an effective way to improve the moisture tolerance of perovskite films via optimal molecular engineering of the interface between the perovskite and HTL. To achieve this goal, only the molecules that meet the following requirements can be chosen: (i) the molecules must have anchor groups that can bind to the surface of $MAPbI_3$; (ii) the molecules should hardly impact the performance of solar cells, as well as the interfacial charge transfer; and (iii) the molecules must be harmless in the formation of the $MAPbI_3$ layer. After systematic screening, an optimal molecule, 1-donecyl mercaptan (NDM), can satisfy all of the demands mentioned above. In the first place, NDM can adsorb on the surface of the $MAPbI_3$ layer by the thiol anchor group of NDM and Pb^{2+} of $MAPbI_3$. In addition, in our experiment, there is no indication that NDM molecules have negative influences on the photovoltaic properties of PSCs. Furthermore, the alkyl chain of the molecules can prevent water molecules from interacting with the $MAPbI_3$ layer, thus enhancing the device tolerance against moisture. It should be noted that the adsorption of NDM molecules on the surface of $MAPbI_3$ might block the interfacial charge transfer in PSCs due to poor conductivity of the alkyl chain. On the contrary, we found that utilizing molecules with a long alkyl chain of 11 C−C bonds to modify the $MAPbI_3$ surface can tune the valence band of $MAPbI_3$, resulting in remarkable improvement in both the efficiency and short-circuit current.

METHODS

Perovskite Film Deposition. The perovskite film was fabricated in ambient air by using a two-step method.[28] First, the annealed TiO_2 nanoparticle film was coated with PbI_2/$PbCl_2$ by spin-coating 0.5 M PbI_2 (99.999%, Aldrich) and 0.15 M $PbCl_2$ (98%, Aldrich) in *N*′,*N*-dimethylformamide (99.7%) at 4500 rpm for 60 s and dried at 100 °C for 15 min. After depositing PbI_2/$PbCl_2$ twice, the perovskite film was made by spin-coating 10 mg/mL CH_3NH_3I (Dyenamo) in 2-propanol at 1200 rpm for 6 s and 4500 rpm for 60 s and dried at 100 °C for 10 min.

Perovskite Solar Cell Fabrication. FTO glasses were cleaned by sequential sonication in deionized water, acetone, and ethyl alcohol. After being treated by UV-ozone for 15 min, the compact TiO_2 layer was deposited immediately by spin-coating 0.15 M titanium tetraisopropanolate in ethyl alcohol at 3000 rpm for 60 s. Then the film was annealed at 500 °C for 2 h. As soon as the film cooled down to room temperature, it was coated with mesoporous TiO_2 (P25) films. After being annealed at 500 °C for 30 min, the perovskite film was formed. The film was dipped in 5 mM NDM chlorobenzene solution for 2 h to adsorb NDM molecules on the surface of $MAPbI_3$. A HTL, consisting of 99.1 mg of spiro-MeOTAD (Lumtec), 0.0395 mL of 4-*tert*-butylpyridine (TBP, 96%, Aldrich), and 11 mg of bis(trifluoromethane) sulfonamide lithium salt (LiTFSI, 99.95%, Aldrich) in 1.4 mL of a mixed solvent of chlorobenzene (99.7%) and acetonitrile (99.7%) (chlorobenzene:acetonitrile, 20:1, v:v), was coated on the perovskite/TiO_2 films by using spin-coating at 4000 rpm for 30 s. Finally, the 80 nm thick Au electrode was deposited on top of the HTL by thermal evaporation at 6.0×10^{-4} Pa vacuum. The device active area was 0.1 cm^2.

Theoretical Modeling and Computational Parameters. First-principles density functional theory calculations were carried out to study the geometry and electronic structure of the perovskite/NDM interface. The static electronic structure was performed with the VASP code by using a plane wave basis, the PBE density functional, and the projector augmented wave (PAW) potentials. An energy cutoff of 500 eV and Γ point k-sampling were used. For geometry optimization of bulk perovskite, a 3 × 3 × 1 Monkhorst−Pack grid was chosen for sampling the Brillouin zone. The calculated lattice constants were $a = b = 6.3115$ Å and $c = 6.3161$ Å for bulk $MAPbI_3$. Our calculated energy gap of bulk $MAPbI_3$ was 1.67 eV, in good agreement with the experimental value of 1.57 eV,[29] due to the cancellation of errors in the exchange−correlation functional and the neglect of spin−orbital coupling (SOC). This cancellation also resulted in a small difference between the results of PBE and GW+SOC or HSE+SOC, verified by many other works on $MAPbI_3$.[29−31] Therefore, in consideration of the huge computational cost, we

DOI: 10.1021/acs.jpcc.8b09722
J. Phys. Chem. C XXXX, XXX, XXX−XXX

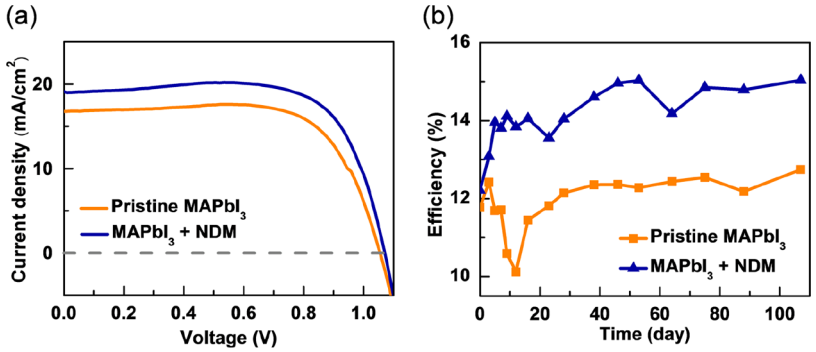

Figure 2. (a) Current−voltage curves of the best PSCs using pristine $MAPbI_3$ (orange curve) and NDM-anchored $MAPbI_3$ (blue curve). (b) Time evolution of the efficiency for the two different devices. The devices were stored in air at room temperature over 100 days out of the sun.

used terse PBE to calculate the geometry and electronic properties of the NDM/$CH_3NH_3PbI_3$ system.

The Γ centered 3 × 3 × 1 Monkhorst−Pack grid was chosen for sampling the Brillouin zone in calculating the ground-state properties of the $MAPbI_3$ slab (Figure 1) and NDM/$MAPbI_3$ interface (Figure 1b,c). For the $MAPbI_3$ slab, the four atomic layers of the halide perovskite was used, and a periodic 1 × 1 supercell was adopted in the parallel $X-Y$ plane. The thickness of the vacuum slab was 10 Å. For the NDM/$MAPbI_3$ heterojunction, we chose NDM molecules bonded at a 4 atomic layer $MAPbI_3$(001) surface terminated with a Pb−I layer (Figure 1c). The atomic geometry was optimized until the forces on nonfixed atoms were below 0.03 eV/ Å. The thickness of the vacuum layer was ∼10 Å to ensure negligible interactions between neighboring slabs.

RESULTS AND DISCUSSION

Influence of NDM Modification on Moisture Stability and Photovoltaic Performance. To investigate the effect of interface engineering on the performance of PSCs, the photocurrent density−voltage ($J-V$) curves (Figure 2a) and the time evolution of the energy conversion efficiency (Figure 2b) of PSCs were measured under 1.5 AM illumination. Surprisingly, both the efficiency and stability of PSCs were enhanced by introduction of NDM molecules. First, the modified PSCs (blue line) showed a significant increase in device performance (Figure 2a). The key parameters of the best devices, including the short-circuit current (J_{sc}), open-circuit voltage (V_{oc}), fill factor (FF), along with the PCE (η) are listed in Table 1. The PCEs of the best modified PSCs reached up to 15.04%, which is 18% higher than that of the best control PSCs (12.75%). The J_{sc}, V_{oc}, and FF of the modified device were all higher than those of the device adopting pristine perovskite. Among them, the short-circuit current was enhanced most significantly, rising from 16.68 mA/cm^2 (controlled PSCs) to 19.06 mA/cm^2 (modified PSCs). We can infer that the addition of NDM molecules is beneficial to the charge transport at the interface or the morphology of perovskite films.

Table 1. Parameters of Best PSCs with and without NDM Molecules

samples	η	J_{sc}	V_{oc}	FF
pristine $MAPbI_3$	12.75	16.68	1.05	72.51
$MAPbI_3$ + NDM	15.04	19.06	1.07	73.15

More importantly, the modified PSCs showed a higher humidity tolerance by real-time monitoring of PCE over a 100 day period. To avoid the influence of varying temperature and light illumination, we shielded them from sun irradiation and tested every 4−5 days at room temperature (Figure 2b). The PCE of the modified PSCs showed rapid growth from 12.21 to 14.12% during the first 10 days, while the PCE of the controlled PSCs decayed from 11.77 to 10.12%. Then, the PCEs of both devices increased gradually and were maintained at ∼15.0% for the modified PSCs and ∼12.5% for the controlled PSCs. Stored in ambient air for over 100 days, the PCE of the modified PSCs increased by 14%, while other PSCs utilizing pristine $MAPbI_3$ showed minimal increases. Therefore, modifying the $MAPbI_3$ surface with hydrophobic NDM molecules can dramatically improve the moisture tolerance of PSCs. On the basis of the structure of NDM molecules, the adsorption geometry on the $MAPbI_3$ surface was carried out as demonstrated in Figure 1c, showing a hydrophobic alkyl chain-packaged perovskite film. The existence of an alkyl chain can keep water molecules away from the surface of $MAPbI_3$, thus improving the stability. Data for reverse scans were not presented in the present work. The readers are directed to previous discussions on the reasons for the hysteresis effect including the influence of interface oxygen vacancies for further studies on that topic.[32−34]

We summarized all of the parameters of PSCs as displayed in Figure 3a. The average efficiency of the modified PSCs was 12.24 ± 1.51%, which is 12% times higher than that of the control (10.96 ± 1.36%). As presented in Figure 3b, the efficiency of ∼20% modified cells exceeded 14%, while the efficiencies of all of the controlled cells were lower than 14%. The comparisons for all device parameters are presented in Figure S1, from which we verified the hypothesis that the enhanced J_{sc} is introduced by adding NDM on the $MAPbI_3$/HTL interface. Therefore, we confirmed the positive impact of NDM molecules on the photovoltaic performance of PSCs.

Influence of NDM Modification on Perovskite Crystallization. To understand the increased efficiency and stability by NDM interface engineering, the XRD patterns for both samples with and without NDM were measured as shown in Figure 4. Both samples were stored in ambient air and shielded from sun irradiation for 34 days. Pristine $MAPbI_3$ showed a negligible peak at 14.8° (red line in Figure 4a), which is assigned to the $MAPbI_3$(110) diffraction. Meanwhile, the modified $MAPbI_3$ showed a more distinct peak at 14.8° (red line in Figure 4b), indicating better crystallization of $MAPbI_3$ with the help of NDM molecules. After storage in ambient air

DOI: 10.1021/acs.jpcc.8b09722
J. Phys. Chem. C XXXX, XXX, XXX−XXX

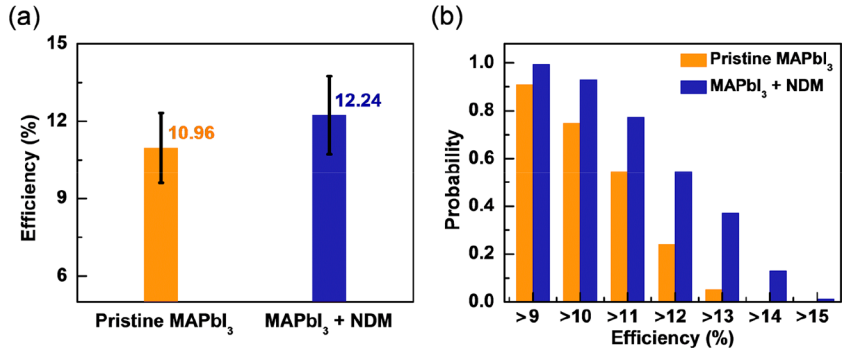

Figure 3. (a) Average efficiency of devices using pristine $MAPbI_3$ (orange) and NDM-anchored $MAPbI_3$ (blue). Error bars represent the mean square error. (b) Cumulative statistical distribution of efficiency among all devices.

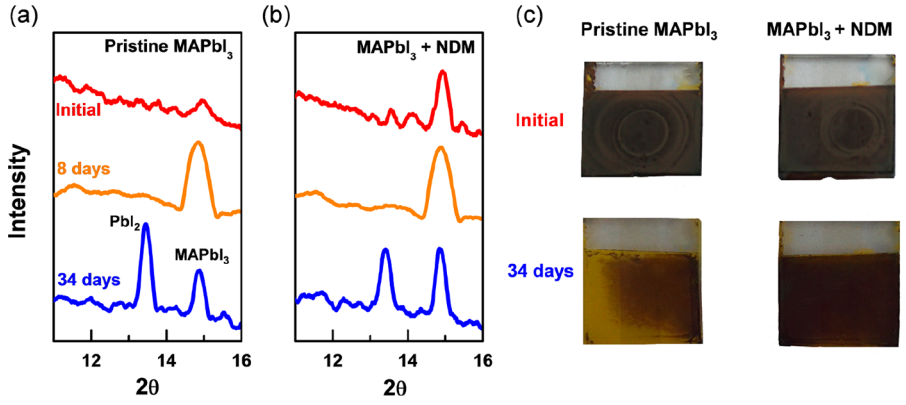

Figure 4. Time-dependent evolution of XRD spectra of pristine $MAPbI_3$ (a) and NDM-anchored $MAPbI_3$ (b) under air condition stored for 0 (red curve), 8 (orange curve), and 34 days (blue curve). (c) Pictures of NDM-anchored $MAPbI_3$ (right) and pristine $MAPbI_3$ (left) deposited on FTO stored in air for 0 (upper) and 34 days (lower).

for 8 days (orange lines in Figure 4a,b), the diffraction peaks at 14.8° of both samples became sharper, demonstrating improved crystal quality of the perovskite layer, possibly due to chemical reactions for 8 days. This increased crystallization of the $MAPbI_3$ layer can dramatically improve light absorption of the active layer and accelerate carrier diffusion in $MAPbI_3$, thus enhancing the photovoltaic performance of the corresponding PSCs. The PbI_2 peaks of both films appeared after storage in ambient air for 34 days (blue lines in Figure 4a,b). However, the PbI_2 peak of the pristine $MAPbI_3$ film was more pronounced than that of the modified film, illustrating that NDM molecules can, to a certain extent, stabilize $MAPbI_3$ by protecting $MAPbI_3$ from degradation in moisture. To exclude the influence of chlorobenzene, samples of the $MAPbI_3$ film dipped in a pure chlorobenzene solution were measured, as presented in Figure S2. By comparing the $PbI_2/MAPbI_3$ ratios after storage in air for 34 days in Figure S3, the decomposition rate follows the order (from high to low) chlorobenzene + $MAPbI_3$ > pristine $MAPbI_3$ > NDM + $MAPbI_3$. Therefore, we conclude that the addition of chlorobenzene accelerates the decomposition of $MAPbI_3$. Consequently, modifying $MAPbI_3$ with NDM molecules not only enhances the antimoisture property of the $MAPbI_3$ perovskite but also leads to better crystallization of the $MAPbI_3$ layer.

The color change of the XRD samples deposited on mesoporous TiO_2 also confirms the protecting role of NDM molecules presented in Figure 4c. The initial colors of both $MAPbI_3$ films were dark brown with no obvious difference between their appearances. After exposure to air for 34 days, the color of pristine $MAPbI_3$ partly faded from dark brown to yellow (PbI_2), whereas the modified $MAPbI_3$ film showed no obvious change in its color. The appearance of circles is due to the boundary of the MAI solution when it was dropped on the surface of PbI_2. We think that the circles are caused by the reaction on the interface of PbI_2, MAI, and air. With the decomposition of $MAPbI_3$, the difference in color fades away gradually.

On the basis of these experiments, we conclude that inserting NDM molecules at the $MAPbI_3$/HTL interface improves the crystallization of $MAPbI_3$ and results in an increase in light harvesting efficiency, thus accelerating carrier diffusion in perovskite films and optimizing the photovoltaic performance of PSCs. Furthermore, it protects the perovskite from degradation in the atmosphere thanks to the hydrophobic properties of the alkyl chain, which improves the long-term stability of PSCs against moisture. The intensities of the perovskite diffraction peaks at 14.8° for both samples stored in air for 8 days were basically the same according to Figure 4a,b. The enhanced crystallization of the perovskite alone cannot fully explain the extensive difference in efficiency. The modified interface suggests that interface engineering on band level alignment caused by NDM molecules plays a significant role, which is discussed below.

Influence of NDM Modification on the Interfacial Electronic Structure. In terms of interface engineering, NDM molecules could enhance the photovoltaic performance of PSCs via the following plausible ways: First, NDM may change the valence band of $MAPbI_3$ via interfacial interactions

DOI: 10.1021/acs.jpcc.8b09722
J. Phys. Chem. C XXXX, XXX, XXX−XXX

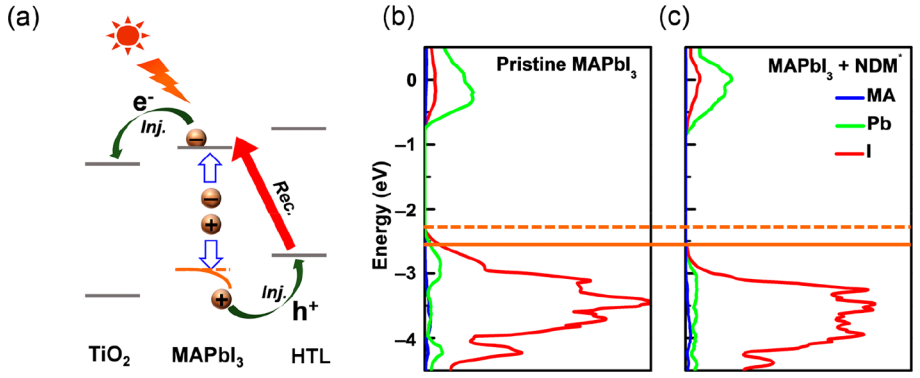

Figure 5. (a) Schematic diagram on the energy level alignment of PSCs and the working principle of solar cells. The orange line is the change of the VBM for the $MAPbI_3$ surface layers before (dash) and after (solid) NDM modification. (b,c) PDOS of pristine $MAPbI_3$ and NDM-anchored $MAPbI_3$; the orange line stands for the VBM at the surface, which shows a downward shift consistent with that in (a).

with perovskite, thus accelerating hole injection. Second, NDM may suppress electron−hole recombination at the $MAPbI_3$/HTL interface, leading to an increased J_{sc}. To investigate the influence of NDM modification on the interfacial electronic structure of PSCs, we investigated the electronic structures of pristine $MAPbI_3$ and NDM*/$MAPbI_3$ by using first-principles calculations (Figure 1b,c). Simplified NDM molecules with a shorter carbon chain length (NDM*) were adopted.

We calculated the alignment of electronic levels of pristine $MAPbI_3$ and NDM*/$MAPbI_3$ systems. Figure 5b,c shows the projected density of states (PDOS) of both systems, where the energy was measured against the vacuum energy level. The DOS was projected on Pb, I, and MA species. It shows that the valence band maximum (VBM) of the perovskite is composed mainly of I atoms, and the conduction band minimum (CBM) of the perovskite is composed mainly of Pb atoms. MA molecules contribute little to the band edge states. The calculated VBM and CBM energies were −2.36 and −0.70 eV for pristine $MAPbI_3$ and −2.57 and −0.77 eV for NDM*-modified $MAPbI_3$, respectively. The energy gap of $MAPbI_3$ increased from 1.66 eV (pristine $MAPbI_3$) to 1.80 eV ($MAPbI_3$ + NDM*), resulting from the effect of surface passivation with NDM* molecules. After introduction of NDM* molecules, the VBM of $MAPbI_3$ (dashed orange line in Figure 5a) shifts downward to a level lower than that of the pristine $MAPbI_3$ (solid orange line in Figure 5a), which is the result of adsorption of the −SH moiety. When the −SH group interacts with Pb^{2+}, the spatial distribution of the electron density near the Fermi level is more delocalized due to the competition in binding Pb^{2+} between −SH and I^-. Because the VBM of $MAPbI_3$ is dominated by I^-, the introduction of −SH could weaken the electronegativity of I^-, thus lowering the VBM of the perovskite.

Considering that NDM molecules were inserted between the $MAPbI_3$ slab and the HTL in PSCs, photogenerated holes might inject from the valence band of $MAPbI_3$ to the HOMO of the HTL. The lowered VBM will accelerate hole injection at the $MAPbI_3$/HTL interface following the Shockley equation

$$J = J_S\left[exp\left(\frac{qV}{k_0T}\right) - 1\right] \qquad \frac{E_F^n - E_F^q}{q} = V$$

The higher energy difference will induce larger photocurrent at the interface by accelerating the injection of carriers. Consequently, modification with NDM at the $MAPbI_3$/HTL interface could effectively improve the photocurrent of PSCs by accelerating the hole injection process, which offsets the negative impact of the enlarged spacing between $MAPbI_3$ and the HTL by adsorption of NDM molecules. In addition, the enlarged spacing may suppress the electron−hole recombination process at the interface.

CONCLUSIONS

We demonstrate that significant improvement in both the stability and PCE of PSCs can be achieved by inserting NDM molecules on the interface of the $MAPbI_3$ slab and HTL. NDM molecules binding to Pb^{2+} of $MAPbI_3$ favor better crystallization of the $MAPbI_3$ layer, enhancing the efficiency of light harvesting and antimoisture stability. More importantly, the introduction of NDM can lower the VBM of $MAPbI_3$ to facilitate the injection of holes due to the enlarged driving force. These results provide a novel perspective for building high-performance PSCs with good air stability through molecular interface engineering, thus accelerating the rapid development of future large-scale practical applications.

ASSOCIATED CONTENT

Supporting Information

The Supporting Information is available free of charge on the ACS Publications website at DOI: 10.1021/acs.jpcc.8b09722.

Average J_{sc}, V_{oc}, and FF of devices, time-dependent evolution of XRD spectra, and PbI_2/$MAPbI_3$ ratios obtained from XRD spectra (PDF)

AUTHOR INFORMATION

Corresponding Authors

*E-mail: guoxf@pku.edu.cn (X.G.).
*E-mail: smeng@iphy.ac.cn (S.M.).

ORCID

Huixia Fu: 0000-0002-4498-6946
Sheng Meng: 0000-0002-1553-1432
Xuefeng Guo: 0000-0001-5723-8528

Author Contributions

L.M. and F.Z. contributed equally to this work.

Notes

The authors declare no competing financial interest.

ACKNOWLEDGMENTS

We gratefully acknowledge financial support from the National Key Research and Development Program of China (Grant No.

DOI: 10.1021/acs.jpcc.8b09722
J. Phys. Chem. C XXXX, XXX, XXX−XXX

2016YFA0300902, 2017YFA0204901, and 2015CB921001), the National Natural Science Foundation of China (Grant No. 11474328 and 11774396), and the "Strategic Priority Research Program (B)" of the Chinese Academy of Sciences (Grant No. XDB07030100).

REFERENCES

(1) Qing, J.; Chandran, H. T.; Cheng, Y. H.; Liu, X. K.; Li, H. W.; Tsang, S. W.; Lo, M. F.; Lee, C. S. Chlorine Incorporation for Enhanced Performance of Planar Perovskite Solar Cell Based on Lead Acetate Precursor. *ACS Appl. Mater. Interfaces* **2015**, *7*, 23110−23116.
(2) Jeon, N. J.; Noh, J. H.; Kim, Y. C.; Yang, W. S.; Ryu, S.; Seok, S. I. Solvent Engineering for High-Performance Inorganic−Organic Hybrid Perovskite Solar Cells. *Nat. Mater.* **2014**, *13*, 897−903.
(3) Stranks, S. D.; Eperon, G. E.; Grancini, G.; Menelaou, C.; Alcocer, M. J. P.; Leijtens, T.; Herz, L. M.; Petrozza, A.; Snaith, H. J. Electron-Hole Diffusion Lengths Exceeding 1 Micrometer in an Organometal Trihalide Perovskite Absorber. *Science* **2013**, *342*, 341−344.
(4) Shi, D.; Adinolfi, V.; Comin, R.; Yuan, M.; Alarousu, E.; Buin, A.; Chen, Y.; Hoogland, S.; Rothenberger, A.; Katsiev, K.; et al. Low Trap-State Density and Long Carrier Diffusion in Organolead Trihalide Perovskite Single Crystals. *Science* **2015**, *347*, 519−522.
(5) Dong, Q.; Fang, Y.; Shao, Y.; Mulligan, P.; Qiu, J.; Cao, L.; Huang, J. Electron-Hole Diffusion Lengths > 175 μm in Solution-Grown $CH_3NH_3PbI_3$ Single Crystals. *Science* **2015**, *347*, 967−970.
(6) Zhou, H.; Nie, Z.; Yin, J.; Sun, Y.; Zhuo, H.; Wang, D.; Li, D.; Dou, J.; Zhang, X.; Ma, T. Antisolvent Diffusion-Induced Growth, Equilibrium Behaviours in Aqueous Solution and Optical Properties of $CH_3NH_3PbI_3$ Single Crystals for Photovoltaic Applications. *RSC Adv.* **2015**, *5*, 85344−85349.
(7) Wang, Z.; Lin, Q.; Chmiel, F. P.; Sakai, N.; Herz, L. M.; Snaith, H. J. Efficient Ambient-Air-Stable Solar Cells With 2D−3D Heterostructured Butylammonium-Caesium-Formamidinium Lead Halide Perovskites. *Nat. Energy* **2017**, *2*, 17135.
(8) Tsai, H.; Nie, W.; Blancon, J.-C.; Stoumpos, C. C.; Asadpour, R.; Harutyunyan, B.; Neukirch, A. J.; Verduzco, R.; Crochet, J. J.; Tretiak, S.; et al. High-Efficiency Two-Dimensional Ruddlesden−Popper Perovskite Solar Cells. *Nature* **2016**, *536*, 312−316.
(9) Wang, D.; Wright, M.; Elumalai, N. K.; Uddin, A. Stability of Perovskite Solar Cells. *Sol. Energy Mater. Sol. Cells* **2016**, *147*, 255−275.
(10) Rajamanickam, N.; Kumari, S.; Vendra, V. K.; Lavery, B. W.; Spurgeon, J.; Druffel, T.; Sunkara, M. K. Stable and Durable $CH_3NH_3PbI_3$ Perovskite Solar Cells at Ambient Conditions. *Nanotechnology* **2016**, *27*, 235404.
(11) *NREL Best Research-Cell Efficiencies*. https://www.nrel.gov/pv/assets/pdfs/pv-efficiency-chart.20190103.pdf (2019).
(12) Yang, W. S.; Park, B.-W.; Jung, E. H.; Jeon, N. J.; Kim, Y. C.; Lee, D. U.; Shin, S. S.; Seo, J.; Kim, E. K.; Noh, J. H.; et al. Iodide Management in Formamidinium-Lead-Halide−Based Perovskite Layers for Efficient Solar Cells. *Science* **2017**, *356*, 1376−1379.
(13) Xiao, M.; Huang, F.; Huang, W.; Dkhissi, Y.; Zhu, Y.; Etheridge, J.; Gray-Weale, A.; Bach, U.; Cheng, Y.-B.; Spiccia, L. A Fast Deposition-Crystallization Procedure for Highly Efficient Lead Iodide Perovskite Thin-Film Solar Cells. *Angew. Chem.* **2014**, *126*, 10056−10061.
(14) Yang, S.; Wang, Y.; Liu, P.; Cheng, Y.-B.; Zhao, H. J.; Yang, H. G. Functionalization of Perovskite Thin Films With Moisture-Tolerant Molecules. *Nat. Energy* **2016**, *1*, 15016.
(15) Leguy, A. M. A.; Hu, Y.; Campoy-Quiles, M.; Alonso, M. I.; Weber, O. J.; Azarhoosh, P.; van Schilfgaarde, M.; Weller, M. T.; Bein, T.; Nelson, J.; et al. Reversible Hydration of $CH_3NH_3PbI_3$ in Films, Single Crystals, and Solar Cells. *Chem. Mater.* **2015**, *27*, 3397−3407.
(16) Li, X.; Ibrahim Dar, M.; Yi, C.; Luo, J.; Tschumi, M.; Zakeeruddin, S. M.; Nazeeruddin, M. K.; Han, H.; Grätzel, M. Improved Performance and Stability of Perovskite Solar Cells by Crystal Crosslinking with Alkylphosphonic Acid ω-ammonium Chlorides. *Nat. Chem.* **2015**, *7*, 703−711.
(17) Chueh, C.-C.; Liao, C.-Y.; Zuo, F.; Williams, S. T.; Liang, P.-W.; Jen, A. K. Y. The Roles of Alkyl Halide Additives in Enhancing Perovskite Solar Cell Performance. *J. Mater. Chem. A* **2015**, *3*, 9058−9062.
(18) Gu, Z.; Zuo, L.; Larsen-Olsen, T. T.; Ye, T.; Wu, G.; Krebs, F. C.; Chen, H. Interfacial Engineering of Self-Assembled Monolayer Modified Semi-Roll-to-Roll Planar Heterojunction Perovskite Solar Cells on Flexible Substrates. *J. Mater. Chem. A* **2015**, *3*, 54254−54260.
(19) Sun, C.; Xue, Q.; Hu, Z.; Chen, Z.; Huang, F.; Yip, H.-L.; Cao, Y. Phosphonium Halides as Both Processing Additives and Interfacial Modifiers for High Performance Planar-Heterojunction Perovskite Solar Cells. *Small* **2015**, *11*, 3344−3350.
(20) Chaudhary, B.; Kulkarni, A.; Jena, A. K.; Ikegami, M.; Udagawa, Y.; Kunugita, H.; Ema, K.; Miyasaka, T. Poly(4-Vinylpyridine)-Based Interfacial Passivation to Enhance Voltage and Moisture Stability of Lead Halide Perovskite Solar Cells. *ChemSusChem* **2017**, *10*, 2473−2479.
(21) Cao, J.; Yin, J.; Yuan, S.; Zhao, Y.; Li, J.; Zheng, N. Thiols as Interfacial Modifiers to Enhance the Performance and Stability of Perovskite Solar Cells. *Nanoscale* **2015**, *7*, 9443−9447.
(22) Park, J. H.; Seo, J.; Park, S.; Shin, S. S.; Kim, Y. C.; Jeon, N. J.; Shin, H.-W.; Ahn, T. K.; Noh, J. H.; Yoon, S. C.; et al. Efficient $CH_3NH_3PbI_3$ Perovskite Solar Cells Employing Nanostructured p-Type NiO Electrode Formed by a Pulsed Laser Deposition. *Adv. Mater.* **2015**, *27*, 4013−4019.
(23) Li, S.-S.; Tu, K.-H.; Lin, C.-C.; Chen, C.-W.; Chhowalla, M. Solution-Processable Graphene Oxide as an Efficient Hole Transport Layer in Polymer Solar Cells. *ACS Nano* **2010**, *4*, 3169−3174.
(24) Manders, J. R.; Tsang, S.-W.; Hartel, M. J.; Lai, T.-H.; Chen, S.; Amb, C. M.; Reynolds, J. R.; So, F. Solution-Processed Nickel Oxide Hole Transport Layers in High Efficiency Polymer Photovoltaic Cells. *Adv. Funct. Mater.* **2013**, *23*, 2993−3001.
(25) You, J.; Meng, L.; Song, T.-B.; Guo, T.-F.; Yang, Y.; Chang, W.-H.; Hong, Z.; Chen, H.; Zhou, H.; Chen, Q.; et al. Improved Air Stability of Perovskite Solar Cells via Solution-Processed Metal Oxide Transport Layers. *Nat. Nanotechnol.* **2016**, *11*, 75−81.
(26) Hwang, I.; Jeong, I.; Lee, J.; Ko, M. J.; Yong, K. Enhancing Stability of Perovskite Solar Cells to Moisture by the Facile Hydrophobic Passivation. *ACS Appl. Mater. Interfaces* **2015**, *7*, 17330−17336.
(27) Xiong, H.; Rui, Y.; Li, Y.; Zhang, Q.; Wang, H. Hydrophobic Coating Over a $CH_3NH_3PbI_3$ Absorbing Layer Towards Air Stable Perovskite Solar Cells. *J. Mater. Chem. C* **2016**, *4*, 6848−6854.
(28) Burschka, J.; Pellet, N.; Moon, S.-J.; Humphry-Baker, R.; Gao, P.; Nazeeruddin, M. K.; Gratzel, M. Sequential Deposition as a Route to High-Performance Perovskite-Sensitized Solar Cells. *Nature* **2013**, *499*, 316−319.
(29) Umari, P.; Mosconi, E.; De Angelis, F. Relativistic GW calculations on $CH_3NH_3PbI_3$ and $CH_3NH_3SnI_3$ Perovskites for Solar Cell Applications. *Sci. Rep.* **2015**, *4*, 4467.
(30) Menéndez-Proupin, E.; Palacios, P.; Wahnón, P.; Conesa, J. C. Self-Consistent Relativistic Band Structure of the $CH_3NH_3PbI_3$ Perovskite. *Phys. Rev. B: Condens. Matter Mater. Phys.* **2014**, *90*, No. 045207.
(31) Agiorgousis, M. L.; Sun, Y.-Y.; Zeng, H.; Zhang, S. Strong Covalency-Induced Recombination Centers in Perovskite Solar Cell Material $CH_3NH_3PbI_3$. *J. Am. Chem. Soc.* **2014**, *136*, 14570−14575.
(32) Zhang, F.; Ma, W.; Guo, H.-Z.; Zhao, Y.-C.; Shan, X.-Y.; Jin, K.-J.; Tian, H.; Zhao, Q.; Yu, D.-P.; Lu, X.-H.; et al. Interfacial Oxygen Vacancies as a Potential Cause of Hysteresis in Perovskite Solar Cells. *Chem. Mater.* **2016**, *28*, 802−812.
(33) Snaith, H. J.; Abate, A.; Ball, J. M.; Eperon, G. E.; Leijtens, T.; Noel, N. K.; Stranks, S. D.; Wang, J. T.-W.; Wojciechowski, K.; Zhang, W. Anomalous Hysteresis in Perovskite Solar Cells. *J. Phys. Chem. Lett.* **2014**, *5*, 1511−1515.
(34) De Bastiani, M.; Dell'Erba, G.; Gandini, M.; D'Innocenzo, V.; Neutzner, S.; Kandada, A. R. S.; Grancini, G.; Binda, M.; Prato, M.;

DOI: 10.1021/acs.jpcc.8b09722
J. Phys. Chem. C XXXX, XXX, XXX−XXX

Ball, J. M.; et al. Ion Migration and the Role of Preconditioning Cycles in the Stabilization of the J−V Characteristics of Inverted Hybrid Perovskite Solar Cells. *Adv. Energy Mater.* **2016**, *6*, 1501453.

DOI: 10.1021/acs.jpcc.8b09722
J. Phys. Chem. C XXXX, XXX, XXX−XXX